Supporting Information

Lithium Intercalation Edge Effects and Doping Implications for Graphite Anodes

Chao Peng,*[a,d,†] Michael P. Mercer,[b,d,†] Chris-Kriton Skylaris,[c,d] and Denis Kramer*[a,d,e]

[a]School of Engineering, University of Southampton, Southampton SO17 1BJ, U. K.
[b]Department of Chemistry, Lancaster University, Bailrigg, Lancaster, LA1 4YB, U. K.
[c]School of Chemistry, University of Southampton, Southampton SO17 1BJ, U. K.
[d]The Faraday Institution, Quad One, Becquerel Avenue, Harwell Campus, Didcot, OX11 0RA, U. K.
[e]Faculty of Mechanical Engineering, Helmut-Schmidt University, Hamburg, 22043, Germany

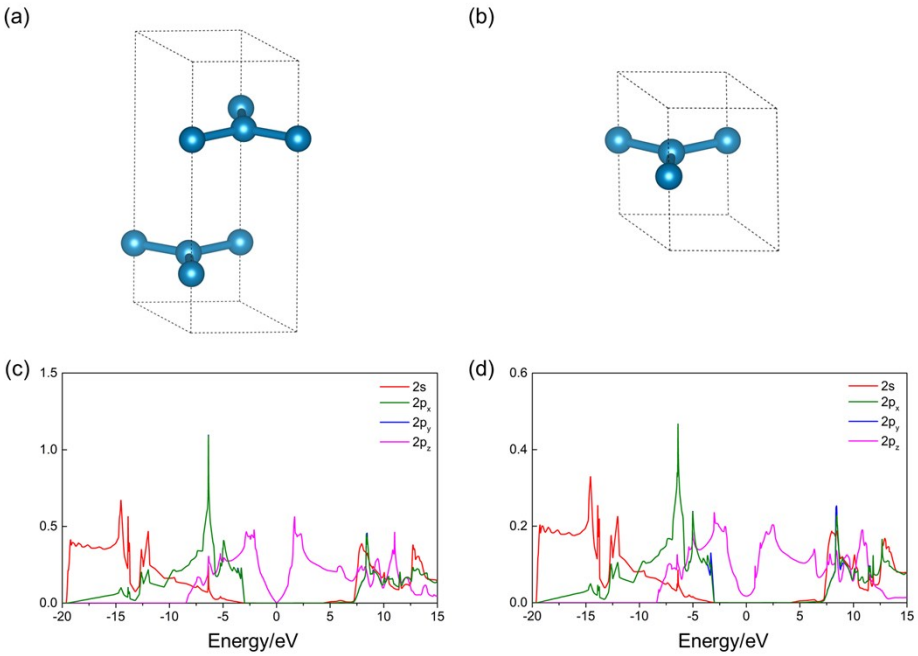

Figure S1. Geometrical and electronic structures of AB and AA stackings of graphite. (a) and (b) are the unit-cells of AB and AA stacking of graphite. (c) and (d) are the projected density of states (pDOSs) of structural (a) and (b), respectively.

Table S1. Optimized and experimental lattice parameters and distances of carbon

interlayers in graphite.

Graphite	d_L/Å	Lattice parameters/ Å		
		a	b	c
AB	3.386	2.466	2.466	6.707
AA	3.441	2.464	2.464	3.441
Exp(AB)[a]	3.386	2.464	2.464	6.771

d_L: the distance of interlayer.

[a]The experimental lattice parameters from Ref. 1.

1. Model construction

Two graphite edges were constructed perpendicular to the basal plane, namely the armchair edge and zigzag edge. The usual slab approach has been used with two equivalent surfaces per unit cell and sufficient vacuum to quench spurious interactions between periodic images. To accurately investigate the influence of the edges on Li adsorption, minimizing the effect of the edge on the opposite side of the cell, we built large supercells where the adsorption energy of Li in the center of a slab is similar to that in bulk graphite as summarized in Table S2. Sufficiently thick slabs were chosen such that the Li site energy difference between edge and slab interior became independent on slab thickness. Accordingly, we selected the armchair-edged supercells with z direction at 27.25 Å and zigzag-edged supercell with z direction at 46.98 Å.

Table S2. Adsorption of Li at different z directions of armchair-edged and zigzag-edged graphite supercells. E_{bulk} and E_{edge} represent Li adsorption at edge and bulk sites, respectively. $\Delta E_{(bulk\text{-}Edge)}$ is the energy difference between E_{bulk} and E_{edge}.

Edges	E_{ads} (Li)/ eV					
Armchair	**Supercells (z /Å)**	27.25	32.17	37.10	42.03	46.96
	$\mathbf{E_{bulk}}$	-0.24	-0.33	-0.33	-0.31	-0.26
	$\mathbf{E_{edge}}$	-0.38	-0.46	-0.48	-0.46	-0.40
	$\mathbf{\Delta E_{(bulk\text{-}Edge)}}$	**-0.14**	**-0.14**	**-0.15**	**-0.15**	**-0.14**
Zigzag	**Supercells (z /Å)**	29.91	34.18	38.45	46.98	60.52
	$\mathbf{E_{bulk}}$	-0.36	-0.36	-0.37	-0.26	-0.26
	$\mathbf{E_{edge}}$	-0.70	-0.74	-0.75	-0.66	-0.66
	$\mathbf{\Delta E_{(bulk\text{-}Edge)}}$	**-0.34**	**-0.39**	**-0.38**	**-0.41**	**-0.40**

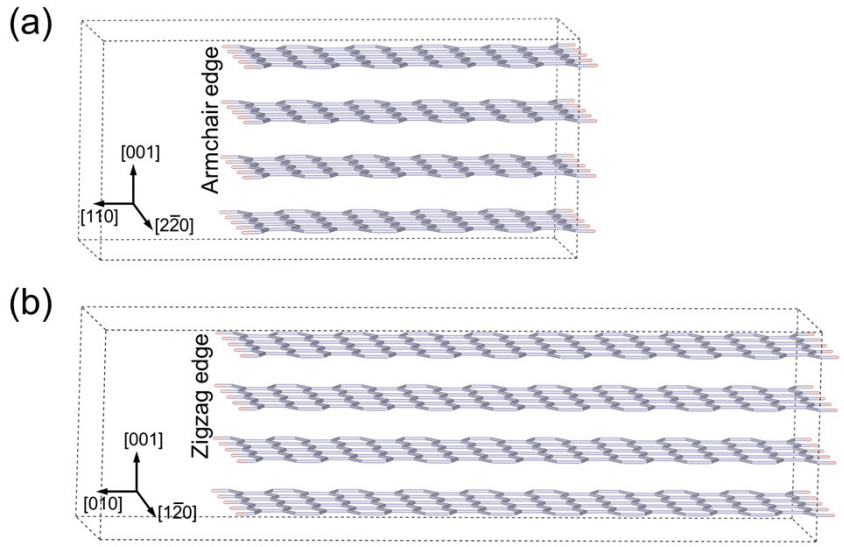

Figure S2. Periodic systems of armchair-edged and zigzag-edged graphite. (a) is structure of hydrogen-terminated armchair-edged graphite (a= 13.76 Å, b = 8.53 Å, c = 27.25 Å; α= β= γ= 90°). (b) is hydrogen-terminated zigzag-edged graphite (a= 13.76 Å, b = 9.86 Å, c = 46.98 Å; α= β= γ= 90°).

2. Dipole effect

Asymmetric slab configurations have been used. (i.e., only one side of a slab is lithiated even there are two equivalent edges in the slabs). Whilst computationally more convenient, this approach bears the risk of spurious dipole interactions between slab images. However, the dipole effect was found to be insignificant in this case as ΔE is quite small (see Table S3).

Table S3. Li adsorption energies at armchair-edged and zigzag-edged graphite. 1Li is one Li adsorption at the edge site of graphite while 2Li means two Li adsorption on two equivalent edges of graphite, respectively. E_{Li_ads} is the adsorption energy per Li atom in graphite. ΔE is the difference of Li adsorption energy between the 1Li and 2Li systems.

Adsorption sites	Armchair			Zigzag		
	E_{Li_ads}/ eV		ΔE/ eV	E_{Li_ads}/ eV		ΔE/ eV
	1Li	2Li		1Li	2Li	
1	-0.13	-0.15	-0.02	-0.66	-0.66	0.00
2	-0.24	-0.26	-0.02	-0.49	-0.48	-0.01
3	-0.38	-0.40	-0.02	-0.26	--	--
4	-0.38	-0.40	-0.02	-0.66	-0.66	0.00
5	-0.23	-0.24	-0.01	-0.49	-0.48	-0.01
6	-0.25	-0.24	0.01	-0.38	-0.38	0.00
7	-0.24	--	--	-0.33	--	--
8	-0.24	-0.20	0.04	-0.26	--	--

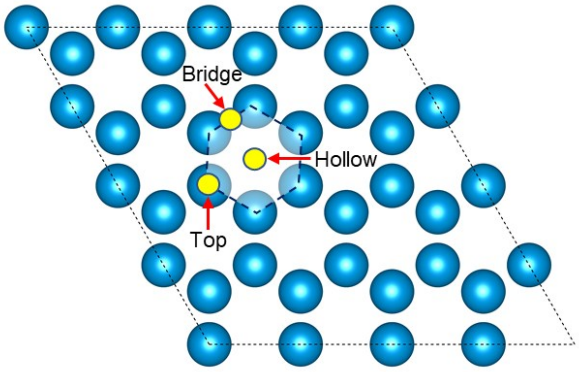

Figure S3. The structure of graphite bulk. The blue circles are carbon atoms and the dashed line is the carbon six-member-ring hexagon in the carbon basal plane. The yellow circles are three possible adsorption sites of Li, namely the top, bridge and hollow sites.

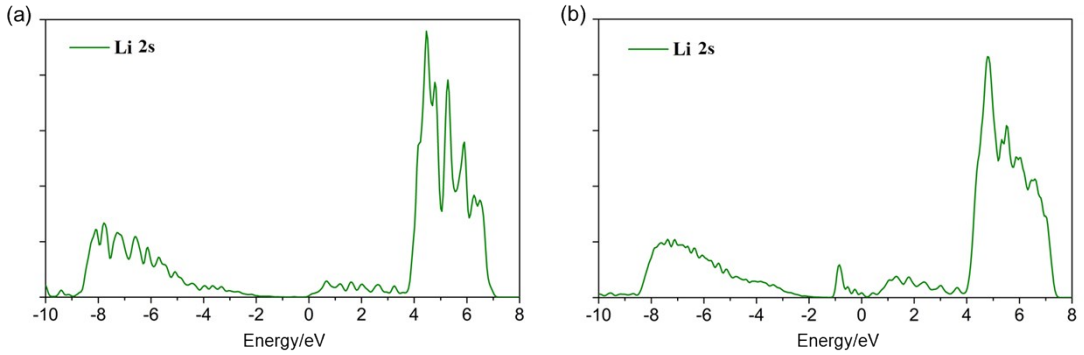

Figure S4. The projected DOS of Li after Li adsorption in (a) armchair-edged and (b) zigzag-edged graphite.

Table S4. Li adsorption energies from the edged site to the bulk site in zigzag-edged graphite with different terminations on edged carbons. The unit is eV.

Adsorption sites	-H	-OH	-F
Edged site	-0.66	-0.30	-0.41
	-0.49	-0.35	-0.38
	-0.38	-0.33	-0.34
	-0.32	-0.30	-0.29
	-0.28	-0.26	-0.27
	-0.26	-0.26	-0.27
	-0.26	-0.27	-0.27
	-0.26	-0.27	-0.27
Bulk site	-0.26	-0.26	-0.27

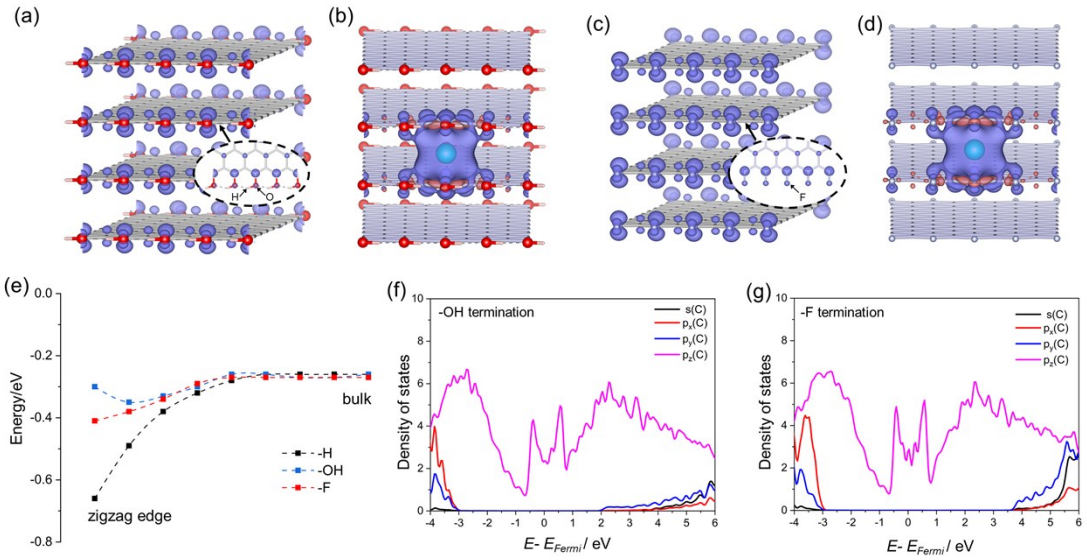

Figure S5. (a) shows the spin density accumulation on the edged carbon in OH-terminated zigzag-edged graphite. The inserted graph shows the top view of the basal plane of graphite edge. The iso-surface value is 0.003 eV/Å^3. (b) is the charge density difference of Li adsorption at the edged site in zigzag-edged graphite. (c) is the spin density in F-terminated zigzag-edged graphite. The inserted graph shows the top view of the basal plane of graphite edge. The iso-surface value is 0.0015 eV/Å^3. (d) is the charge density difference of Li adsorption at the edged site in F-terminated graphite. The iso-surface value is 0.001 eV/Å^3. (e) shows Li adsorption energy change from the edged site to the bulk site in zigzag-edged graphite with different terminations on edged carbons. (f) and (g) are the local density of states (LDOSs) of edged carbons in OH-terminated and F-terminated zigzag-edged graphite.

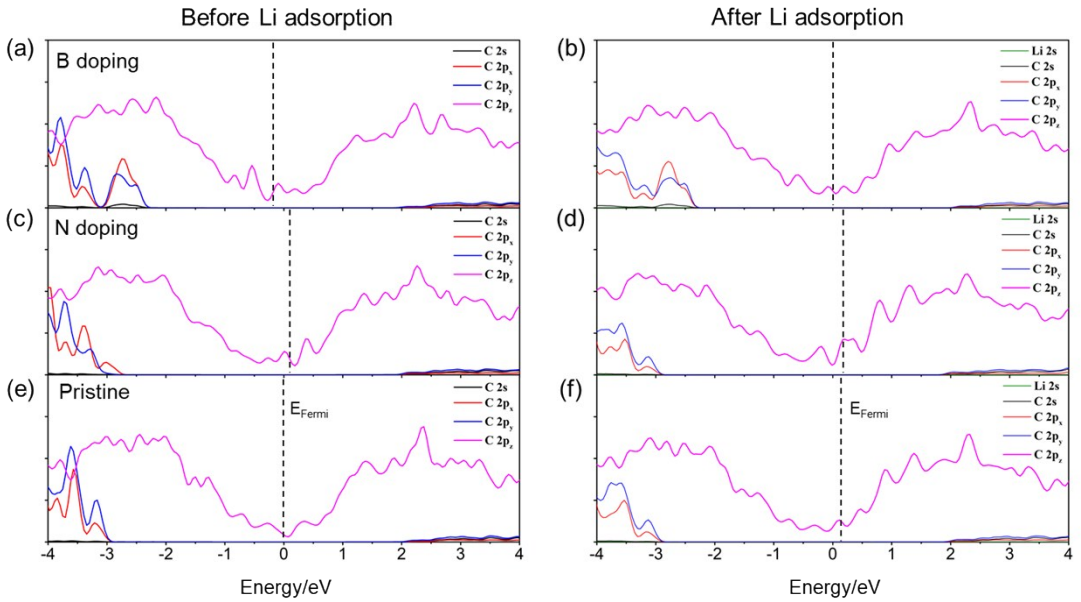

Figure S6. The LDOSs of Li adsorption at the armchair-edged graphite. (a) is the LDOS of edge carbons in boron(B)-doped armchair system. (c) and (d) are LDOSs of edged carbons in nitrogen(N)-doped and pristine armchair system. (b), (d) and (e) are LDOSs of corresponding system with Li adsorption.

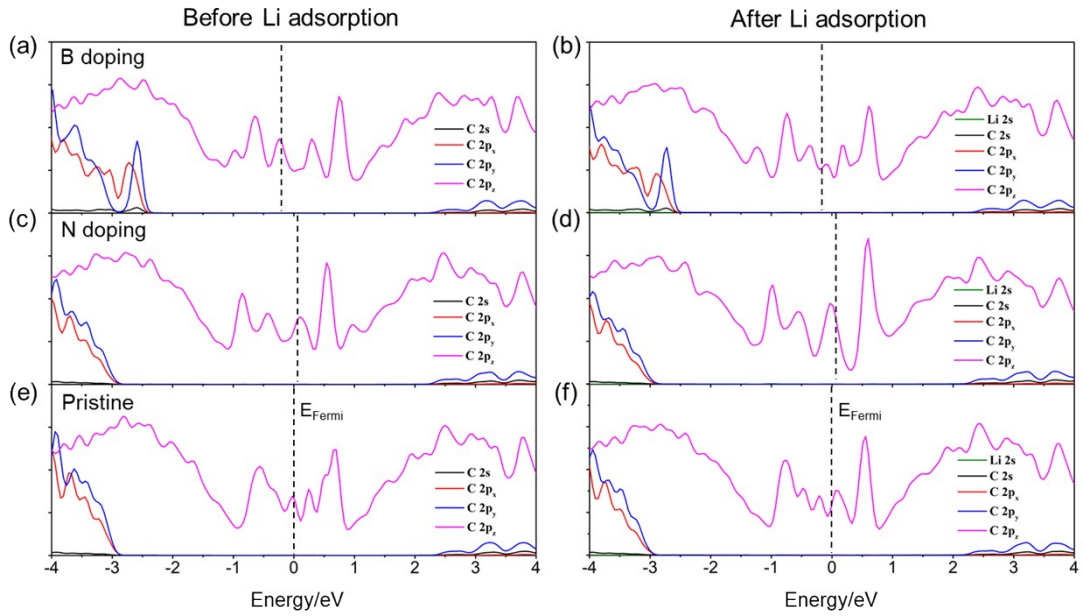

Figure S7. The LDOSs of Li adsorption at the zigzag-edged graphite. (a) and (c) are LDOSs of edged carbons in boron and nitrogen-doped zigzag system. (e) is the LDOS of edge carbons in pristine zigzag system. (b), (d) and (f) are LDOSs of corresponding system with Li adsorption.

Table S5. Li adsorption at the edge of pristine, N and B doped in armchair and zigzag-edged graphite. The N and B were doped in the bulk site of graphite. E_{ads} is Li adsorption energy.

Edges		E_{ads}/eV
armchair	N dope	-0.34
	Pristine	-0.38
	B dope	-0.58
zigzag	N dope	-0.62
	Pristine	-0.66
	B dope	-0.67

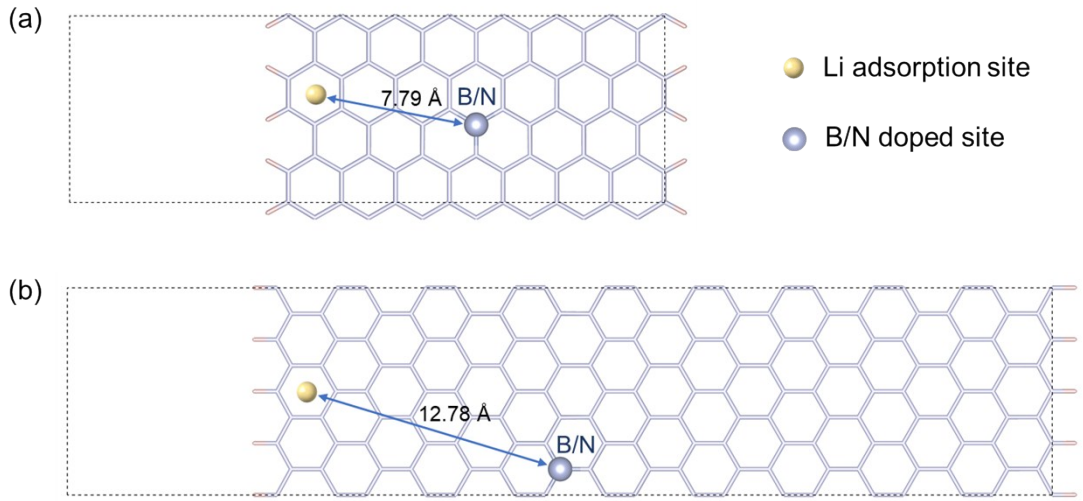

Figure S8. B and N doping at the bulk sites of armchair and zigzag edged systems. (a) shows the bulk-doping site of armchair-edged system, and (b) illustrates the bulk-doping site in zigzag-edged system.

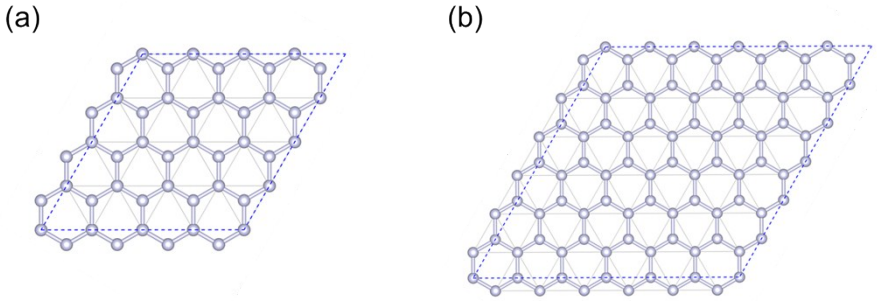

Figure S9. Structures of two graphite bulk with four graphene layers. (a) Bulk 1 (a=b=9.86 Å, c= 13.76 Å) has 128 C atoms. (b) bulk 2 (a=b=14.78 Å, c= 13.76 Å) contains 288 C atoms.

3. Markov chain

A simplified Markov chain model was used to investigate the Li dynamics near the edges. The transition matrix **P** was constructed according to

$$P_{i,j} = \exp\left\{-\frac{\Delta E^{a}_{i,j}}{kT}\right\} \quad (1)$$

Activation energies for jumps from site *i* to *j* ($\Delta E^{a}_{i,j}$) were obtained from nudged-elastic-

band calculations, but the transition states showed mostly a constant offset of approximately 450 meV above the averaged site energies, allowing to express activation energies as:

$$\Delta E_{i,j}^{a} = \left(\frac{E_i + E_j}{2} + 450\ meV\right) - E_i \tag{2}$$

with the exception of a jump from the surface site to the first sub-surface site near the zigzag edge, where an offset of 210 meV was used.

Simulations were performed at room temperature (i.e., $kT = 25\ meV$) over a domain consisting of 20 sub-surface sites. Probability distributions were initialized as

$$\mu_i^{[0]} = \begin{cases} 1 & i = 0 \\ 0 & i \neq 0 \end{cases} \tag{3}$$

with $i = 0$ designating the surface site and propagated in time (t) according to

$$\mu^{[t+1]} = P\mu^{[t]} \tag{4}$$

References:

1 P. Trucano; R. Chen. *Nature* 1975, **258**, 136-137.